International Journal of Nanoelectronics and Materials
Volume 13, No. 1, Jan 2020 [159-168]

The Effects of Titanium Dioxide (TiO_2) and Reduced Graphene Oxide (rGO) Doping Ratio Variation to the Performance of Dye-Sensitized Solar Cell (DSSC)

Afiqah Baharin[1,*], Siti Kudnie Sahari[1], Rafidah Kemat[1] and Najwa Ezira Ahmed Azhar[2]

[1]*Faculty of Engineering, Universiti Malaysia Sarawak (UNIMAS), 94300 Kota Samarahan, Sarawak.*
[2] *NANO-SciTech (NST), Institute of Science, Universiti Teknologi MARA (UiTM), 40450 Shah Alam, Selangor.*

Received 21 June 2019, Revised 8 October 2019, Accepted 31 December 2019

ABSTRACT

The Titanium Dioxide (TiO_2)-reduced Graphene Oxide (rGO) were synthesized and doped at different concentration of 0.1wt%, 0.3wt% and 0.5wt% by varying the amount of rGO solution. The TiO_2 nanoparticles were prepared via precipitation peptization method while rGO solution was prepared via chemical reduction and deposited by using Doctor Blade technique. The TiO_2-rGO thin films samples were characterized by X-ray Diffraction (XRD) spectroscopy and Ultraviolet-visible spectroscopy (UV-Vis) for structural and optical properties while electrical properties were characterized by Keithley sourcemetre. It is observed that all of the TiO_2-rGO samples possess the anatase TiO_2 crystallinity phase which strongly appeared at (101), (004), (200) and (105) peaks and as the amount of rGO increases, the intensity of the peaks decreases. Meanwhile, 0.1wt% of TiO_2-rGO has the highest absorbance wavelength with the lowest bandgap at 2.75 eV which due to formation of Ti-O-C bond. These were confirmed by the efficiency obtained by the 0.1wt% of TiO_2-rGO at 1.21% which is higher than pure TiO_2. The results obtained confirmed that the properties of TiO_2-rGO and performances of DSSC were affected by the doping ratio.

Keywords: Chemical Reduction, Doped, Precipitation-Peptization, Reduced Graphene Oxide, Titanium Dioxide.

1. INTRODUCTION

Recently, there is strong interest in the third generation of photovoltaic solar cell technology, especially the Dye-Sensitized Solar Cell (DSSC) device due to several benefits which include high energy conversion, flexibility, cheap and easy to fabricate as compared to silicon-based solar cells [1,2]. DSSC has a sandwich configuration consisting of photoanode, electrolyte, dye and counter electrode [3,4]. There are many works that have been done to increase the performance of DSSC which include developing new sensitizers, and different counter electrode and photoanode. The photoanode has received great attention due to its function to transport photo-induced electrons and absorb dye which helps to determine the photo-current density [5].

Among various semiconductor, TiO_2 has been widely used as photoanode in DSSC due to its higher photoactivity, wide bandgap of 3.2 eV, low cost and relative non-toxicity [5]. The TiO_2 photoanode has the main role throughout the conversion of light energy to electrical in DSSC. The excited electrons will flow across the Fluorine doped Tin Oxide (FTO), external load and finally to the counter electrode [6]. However, charges recombination is the main factor that limits the performance of DSSC [7] because the back-electron transfer in TiO_2 photoanode-electrolyte

*Corresponding author: *afiqahb94@gmail.com*

interface before reaching the FTO is considered to be the major recombination pathway, which decreases the performance of DSSC [8]. This problem can be solved by using the composite semiconductor photoanode with different bandgaps and some doping elements in TiO_2 photoanode [6]. In the past two decades, Carbon Nanotubes (CNTs) and graphene sheets have doped with TiO_2 photoanode to increase the performance of DSSC [9]. The graphene may be more suitable than CNTs for charge separation due to its large surface area, high electron mobility (15000 $cm^2/V/s$), and good contact with metal oxides [10]. Therefore, rGO is the potential candidate to be coupled with TiO_2 as photoanode in DSSC since graphene has zero bandgap [11]. It helps to generate the electron and hole pairs (EHPs) for high conversion efficiency, lengthy visible light absorption and increase the performance of DSSC. In this present work, TiO_2 doped rGO was prepared with different weight which are 0.1wt%, 0.3wt% and 0.5wt%. The N719 dye will be used as sensitizers. The annealing temperature for the thin film is fixed at 450°C.

2. EXPERIMENTAL METHODS

2.1 Materials

The chemical used during the experiment were Titanium (IV) Isopropoxide (TTIP), propanol (C_3H_8O) and dimethylformamide (DMF) supplied by Sigma Aldrich. Graphene oxide (GO) and Triton X-100 were purchased from R&M Chemicals whereas acetic acid and absolute ethanol were purchased from Fisher Scientific. The chemicals were used without any further purification and entire chemicals were analytical reagents (AR).

2.2 Synthesis of TiO_2

TiO_2 were synthesized via a method of precipitation-peptization utilizing Titanium (IV) Isopropoxide (TTIP) as the precursor. Firstly, beaker A was prepared by adding 10 mL of TTIP into 40 mL of propanol. Then, the solution was continuously stirred for 30 minutes at room temperature. In beaker B, 5 mL of acetic acid, 10 mL of propanol and 100 µL of Triton X-100 were added into 10 mL deionized water. After that, the solution was stirred continuously for 30 minutes at room temperature. Next, the solution in beaker A was added slowly into beaker B with 1 mL/min rate based on previous research [1]. Lastly, the mixture solution was heated on a hot plate at 60°C and stirred at 600 rpm for two hours then left to cool down overnight to surmount the bubbles in the solution.

2.3 Synthesis of rGO

RGO solution was prepared via chemical reduction with graphene oxide (GO) as precursor and hydrazine hydrate as a reduction agent. Initially, 2 mL of GO was added into 100 mL of deionized water and sonicated for 10 minutes. Then, the solution was transferred into a round bottom conical flask and synthesized by using reflux method in an oil bath. After that, 17 µL of hydrazine hydrate was immediately added into the GO solution as soon as the heating started. The solution was then stirred on the hot plate at 80°C with 300 rpm stirring speed for 12 hours resulting black colour liquid. To acquire the rGO powder, the solution was filtered by using a filter membrane to remove the excess water and left to dry for another 12 hours. Next, 40 mL of dimethylformamide (DMF) which act as the solvent was added to 1.5 gram of rGO powder to form rGO solution. Lastly, the solution was sonicated for 15 minutes until entire rGO powder was fully dissolved in DMF.

2.4 Preparation of TiO_2 Doped rGO

TiO_2 was doped with different volumes of rGO and the doping weight were set at 0.1wt%, 0.3wt% and 0.5wt%. For 0.1wt% TiO_2-rGO, 6 mL of rGO solution was mixed with 60 mL of TiO_2 solution in a beaker and stirred continuously for 15 minutes. The steps are repeated for both 0.3wt% and 0.5wt% TiO_2-rGO with different volume of rGO as depicted in Table 1.

Table 1 Volume of TiO_2 and rGO

TiO_2-rGO (wt%)	Volume of TiO_2 (mL)	Volume of rGO (mL)
0.1	60	6
0.3	60	18
0.5	60	30

Next, the mixture was heated on the hot plate at 100°C for 3 hours [1]. Once the powder was fully dried, the powder was annealed at 450°C for 2 hours in the furnace. Then, 100 µL of deionized water was mixed with the TiO_2-rGO powder to form a paste. After that, the paste was deposited on the conductive side of FTO glass by using Doctor Blade method.

2.5 Fabrication of DSSC

The anode and cathode were prepared in order to fabricate DSSC. The FTO substrate coated with 0.1wt% TiO_2-rGO acts as a cathode while the substrate coated with graphite acts as an anode. For the dye preparation, N-719 dye was mixed with 25 mL of absolute ethanol. The substrates were soaked in the dye solution and left overnight to allow the dye to be absorbed by the sample surface. Then, both of the substrates were combined together with a binder clip as shown in Figure 1. A few drops of electrolyte which are Potassium Iodide (KI) were injected between the substrates. The electrical characterization was analysed immediately after the fabrication was done.

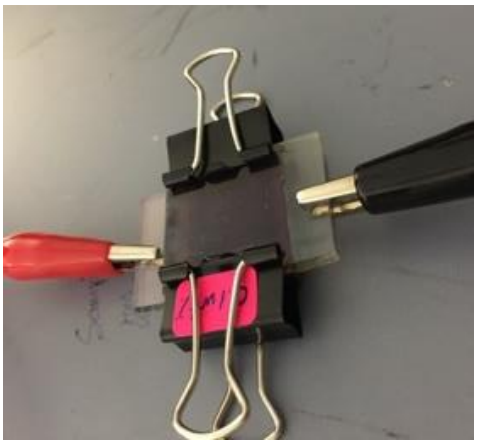

Figure 1. DSSC device.

2.6 Characterization

The X-ray diffraction spectroscopy (XRD, PANalytical X'PERT PRO MRD PW 3040) was used to determine the phase structure of a crystalline material in TiO_2-rGO. The scanning rate employed

was 0.033°s^{-1} in 2Θ range from 20° to 80° with Cu-Kα radiation (λ=1.5406 Å). Next, the absorption spectra of the samples were determined by Ultraviolet spectroscopy (UV-Vis, SHIMADZU UV-1800 UV-Visible Series). The measured absorbance wavelength was set to 200 nm to 800 nm. Lastly, the electrical properties of TiO_2-rGO were obtained by using Keithley Sourcemetre (Model 2450). The measured data from Keithley were presented as current-voltage (I-V) graph.

3. RESULTS AND DISCUSSION

3.1 X-ray Diffraction (XRD)

The XRD pattern of TiO_2-rGO nanoparticles were obtained at different doping ratio as shown at diffraction peak of 2θ = 25.3°, 37.9°, 47.9°, 54.0°, 55.3°, 62.5°, 68.9°, 70.5° and 75.3°. This can be assigned to (101), (004), (200), (105), (211), (204), (116), (220) and (215) that corresponds to anatase phase of titania agrees with (JCPDS card no: 21-1272) [12; 1]. Figure 2 shows the XRD patterns of TiO_2 and TiO_2-rGO nanocomposites subjected to annealing temperature at 450°C. The characteristics peak of rGO could not be observed due to the minimal volume of rGO to be tracked by XRD and it is shadowed by the main peak of anatase TiO_2 at (101) which is consistent with the previous research [13]. In addition, the absence of rGO peak may be due to the high crystallinity of TiO_2 [11,14]. It could be observed that the intensity of the diffraction peak is decreasing when the amount of rGO increased. There are no other contamination peaks detected hence implies that a high purity of TiO_2 nanoparticles was synthesized as shown in the previous study [8].

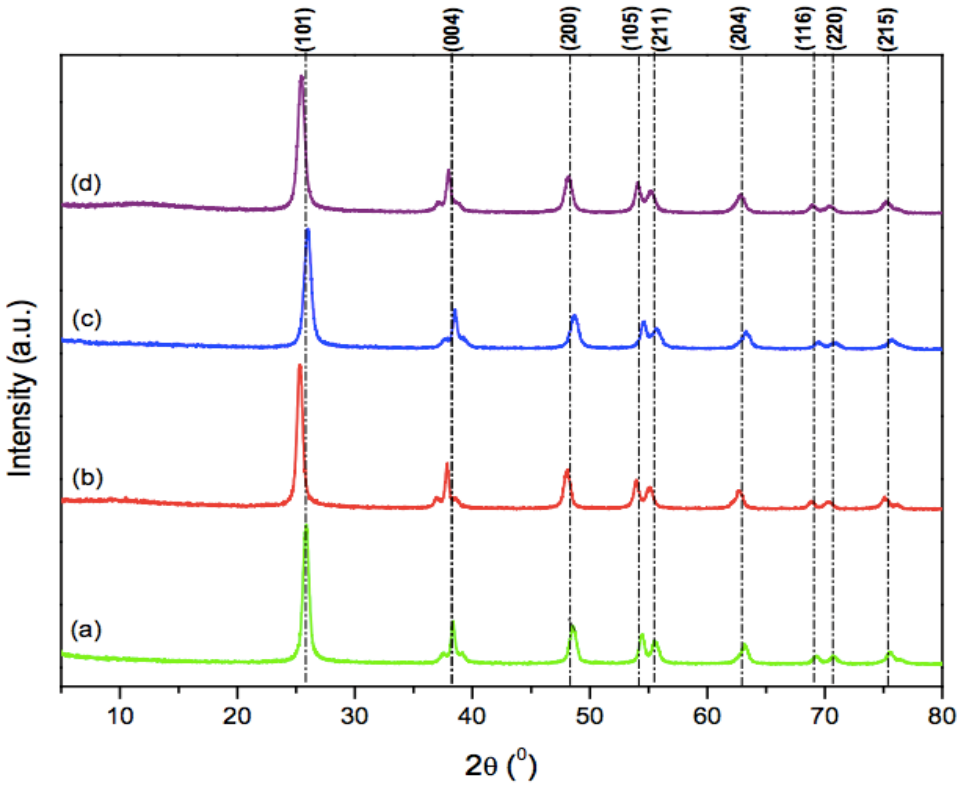

Figure 2. XRD analysis of (a) TiO_2, (b) 0.1wt% TiO_2-rGO, (c) 0.3wt% TiO_2-rGO and (d) 0.5wt% TiO_2-rGO.

The average crystalline particle size is calculated by applying Scherer expressions in Equation (1):

$$D = \frac{0.9\,\lambda}{\beta \cos(\theta)} \quad (1)$$

where λ is the x-ray wavelength (1.5406 Å-Cu K α radiation), β is the line broadening at half maximum intensity (FWHM) and θ is the Bragg angle. The obtained particle size are shown in Table 2. The 0.1wt% TiO_2-rGO shows the smallest average particle size in relation to the highest crystallinity compared to other samples. Nouri and his team reported that the widening of Full Width at Half Maximum (FWHM) of the strongest peak at (101) might be due to the smallest crystalline size [15,16]. According to the TiO_2-rGO NC, 0.1wt% TiO_2-rGO is assumed to have the highest intensity which indicates the best crystalline structure causing the decrement in the bandgap material.

Table 2 The average particle size of the sample

Sample	2θ (°)	FWHM	Average particle size (nm)
TiO_2	25.87	0.6071	14.87
0.1wt% TiO_2-rGO	26.01	0.7032	12.63
0.3wt% TiO_2-rGO	25.32	0.5858	15.12
0.5wt% TiO_2-rGO	25.44	0.6926	13.17

3.2 Ultraviolet-Visible (UV-Vis) Spectroscopy

The comparison for absorbance wavelength of pure TiO_2, 0.1wt% TiO_2-rGO, 0.3wt% TiO_2-rGO and 0.5wt% TiO_2-rGO is shown in Figure 3. It is clearly shown that 0.1wt% TiO_2-rGO is shifted to higher wavelength in the absorbance edge. This will enhance the visible light absorption due to the incorporation of graphene compared to 0.5wt% TiO_2-rGO. This shows that the presence of rGO affects the optical properties of TiO_2-rGO. The decreasing in bandgap energy for TiO_2-rGO NC shows a decrease in charge carrier recombination compared to pure TiO_2.

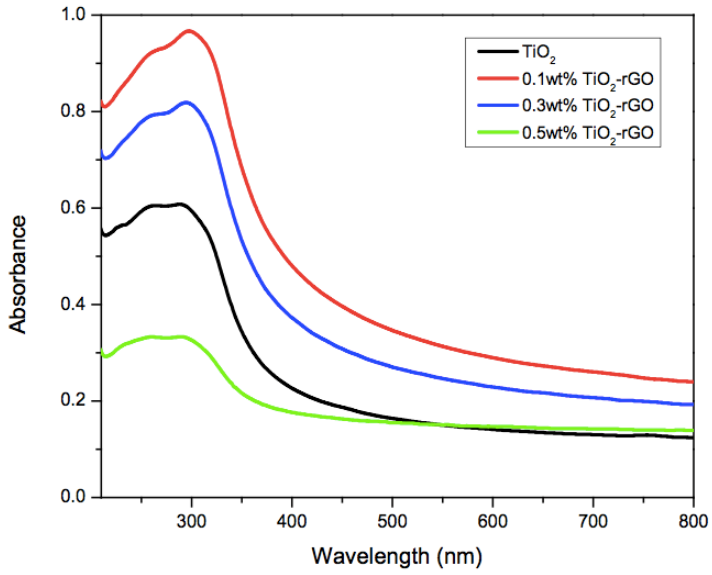

Figure 3. UV-Vis spectroscopy of TiO_2 and different doping ratio of TiO_2-rGO.

In order to obtain the bandgap, the UV-Vis spectra must be converted into Tauc Plot by using the Kubelka-Munk (K-M) formula as in Equation (2):

$$\alpha h\nu = A(h\nu - E_g)^2 \quad (2)$$

Where α is absorbance coefficient, *h* is the plank's constant (4.136 x 10^{-15} eV), *A* is the constant (~1), *v* is the speed of light (3 x 10^8 ms^{-1}), E_g is the bandgap energy and *n* is the indirect allowed transition (2). Table 3 shows the bandgap energy for TiO_2, 0.1wt% TiO_2-rGO, 0.3wt% TiO_2-rGO and 0.5wt% TiO_2-rGO. The 0.1wt% TiO_2-rGO shows the smallest bandgap energy of 2.75 eV might be due to the formation of Ti-O-C bond formed between Ti^{4+} and rGO nanosheets during the doping process [15]. The smaller the bandgap implies a better formation of Ti-O-C bond between TiO_2 and rGO NC [17].

Table 3 Bandgap energy for all samples

Sample	Bandgap Energy (eV)
TiO_2	3.07
0.1wt% TiO_2-rGO	2.75
0.3wt% TiO_2-rGO	2.87
0.5wt% TiO_2-rGO	2.91

3.3 I-V Plot

The DSSC performance of pure TiO_2 and TiO_2-rGO with different concentration are shown in Figure 4. Table 4 shows the photovoltaic characteristics of DSSC such as short circuit current (J_{sc}), open-circuit voltage (V_{oc}), fill factor (FF) and efficiency (η). It can be observed that 0.1wt% TiO_2-rGO achieved the highest power conversion efficiency of 1.21% with J_{sc} of 0.049 A/cm^2, V_{oc} of 0.6 V, and FF of 0.612. The highest V_{oc} obtained might be due to shifting of the energy band of TiO_2 that helps the excited electron to reach the conduction band of FTO which results in accumulation of injected electrons [18]. The value of FF of the solar cell indicates the improved of electron lifetime [19].

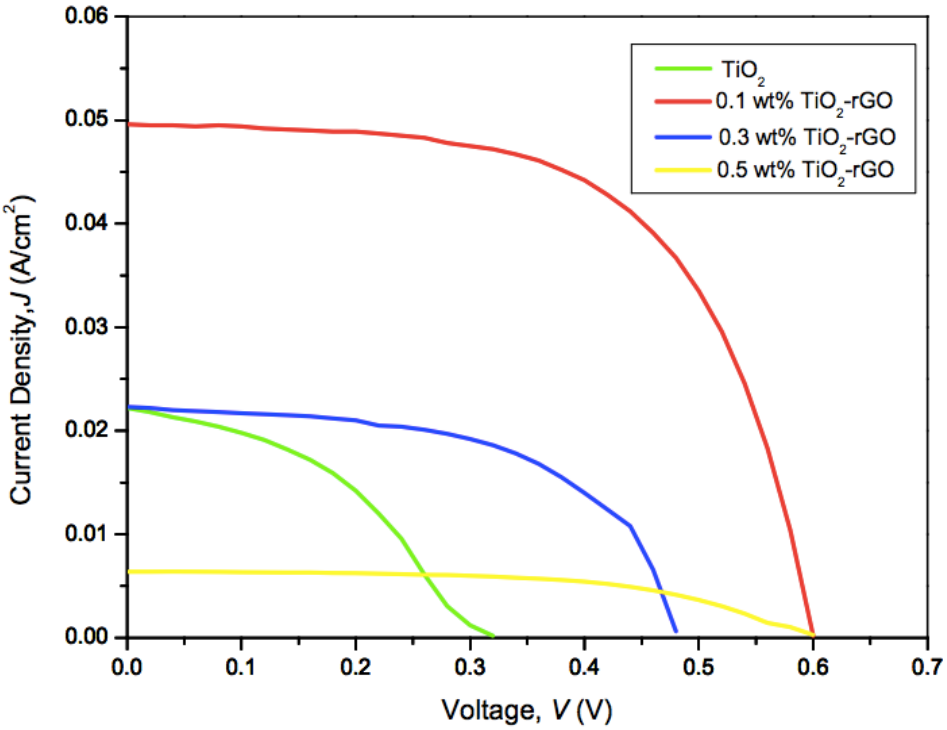

Figure 4. J-V curve of DSSC

The following Equation (3) and (4) are the formulas to calculate the fill factor (FF) and efficiency (η):

$$\eta = \frac{P_{max}}{P_{in}} = \frac{I_{mp}V_{mp}}{P_{in}} = \frac{I_{sc}V_{oc}FF}{P_{in}} \quad (3)$$

$$FF = \frac{V_{mp}I_{mp}}{I_{sc}V_{oc}} \quad (4)$$

where P_{max} is the maximum power, P_{in} is the input power, I_{mp} is the maximum current, V_{mp} is the maximum voltage, V_{oc} is the open-circuit voltage, I_{sc} is the short circuit current and FF is the fill factor. As observed in Table 4, the efficiency of 0.3wt% TiO_2-rGO is still higher than pure TiO_2 but lower than 0.1wt% TiO_2-rGO (1.21%). The initial increase of efficiency is due to the enhancement of electronic conductivity from the increased amount of rGO used in the doping process [20,12]. However, 0.5wt% of TiO_2-rGO has the lowest power conversion efficiency of 0.14% with V_{oc} of 0.6 V, J_{sc} of 0.006 A/cm^2 and FF of 0.583. This might be due to the excessive amount of rGO which might act as recombination centres for photo-induced charge carriers that can lead to a lower sensitivity of solar simulation [21,22]

Table 4 Photovoltaic characteristics of DSSC

Samples	Short circuit current density, I_{sc}/J_{sc} (A/cm^2)	Open circuit voltage, V_{oc} (V)	Fill factor, FF	Efficiency, %
Pure TiO_2	0.022	0.320	0.409	0.19
0.1wt% TiO_2-rGO	0.049	0.600	0.612	1.21
0.3wt% TiO_2-rGO	0.022	0.480	0.547	0.39
0.5wt% TiO_2-rGO	0.006	0.600	0.583	0.14

4. CONCLUSION

This research has demonstrated the preparation of TiO_2 and rGO solution for doping process of TiO_2-rGO. The structural, optical and electrical properties of TiO_2-rGO are fully characterized. The structural properties of TiO_2-rGO indicate that the doping of rGO maintains the crystallinity structure of anatase TiO_2. For optical properties, the doping of rGO enhances the photocatalytic activity by reducing the bandgap of TiO_2-rGO. This can be proved by 0.1wt% TiO_2-rGO shows the smaller bandgap of 2.75 eV compared to pure TiO_2, 3.07 eV. 0.1wt% TiO_2-rGO shows the ideal sample acts as photoanode in DSSC which results in the highest electrical properties in this research.

ACKNOWLEDGEMENT

The author would like to thank Ministry of Higher Education, Malaysia, Fundamental Research Grant Scheme (FRGS/1/2017/STG07/UNIMAS/02/2) and Universiti Malaysia Sarawak (F02/FRGS/1617/2017) for supporting this work.

REFERENCES

[1] F. W. Low, C. W. Lai & S. B. Abd Hamid, "Study of reduced graphene oxide film incorporated of TiO_2 species for efficient visible light driven dye-sensitized solar cell," Journal of Material Science **28**, (2017) 3819-3836.

[2] S. K. Sahari, M. Sawawi, M. Kashif, A. Baharin, R. Kemat & E. Jaafar, "Sensitization of TiO_2 Thin Film with Different Dye for Solar Cell Application," Journal of Telecommunication, Electronic and Computer Engineering (JTEC) **9**, 3-10 (2017) 49-52.

[3] J. Sheng *et al.,* "Characteristics of dye-sensitized solar cells based on the TiO_2 nanotube/nanoparticle composite electrodes," Journal of Material Chemistry **21**, 14 (2011) 5457-5463.

[4] Y. S. Jin *et al.,* "The effect of RF-sputtered TiO_2 passivating layer on the performance of dye sensitized solar cells," Ceramics International **38**, (2012) S505-S509.

[5] A. N. B. Zulkifli, T. Kento, M. Daiki & A. Fujiki, "The Basic Research on the Dye-Sensitized Solar Cell" **3**, 5 (2014) 382-388.

[6] A. Eshaghi & A. A. Aghaei, "Effect of TiO_2-graphene nanocomposite photoanode on dye-sensitized solar cell performance," Bullletin of Material Science **38**, 5 (2015) 1177-1182.

[7] F. W. Low & C. W. Lai, "Recent development of graphene-TiO_2 composite nanomaterials as efficient photoelectrodes in dye-sensitized solar cells," Renewable and Sustainable Energy Reviews **82**, (2018) 103-125.

[8] F. W. Low & C. W. Lai, "Reduced Graphene Oxide decorated TiO_2 for Improving Dye-Sensitized Solar Cells (DSSCs)," Current Nanoscience **14**, (2018) 1-6.

[9] F. W. Low, C. W. Lai & S. B. Hamid, "One-step Hydrothermal synthesis of titanium dioxide decorated on reduced graphene oxide for dye sensitized solar cells application," International Journal of Nanotechnology **15**, 1/2/3 (2018) 78-92.

[10] F. W. Low, C. W. Lai & S. B. Hamid, S. Chong & W. W. Liu, "High Yield Preparation of Graphene Oxide Film Using Improved Hummer's Technique for Current-Voltage Characteristics," Advanced Material Research **1109**, (2015) 385-389.

[11] C. W. Lai, F. W. Low, S. W. Chong, C. P. Wong, S. Z. Siddick, C. J. Juan & S. B. Hamid, "An Overview: Recent Development of Titanium Dioxide Loaded Graphene Nanocomposite Film for Solar Application," Current Organic Chemistry **19**, 19 (2015) 1882-1895.

[12] J. Zhang, Z. Xiong & X. S. Zhao, "Graphene-metal-oxide composites for the degradation of dyes under visible light irradiation," Journal of Materials Chemistry **21**, 11 (2011) 3634-3640.

[13] H. Ding, S. Zhang, J. T. Chen, X. P. Hu, Z. F. Du, Y. X. Qiu & D. L. Zhao, "Reduction of graphene oxide at room temperature with vitamin C for rGO-TiO_2 photoanodes in dye sensitized solar cell," Thin Solid Films **584**, (2015) 29-36.

[14] J. S. Lee, K. H. You & C. B. Park, "Highly proactive, low bandgap TiO_2, nanoparticles wrapped by graphene," Advanced Materials **24**, (2012) 1084-1088.

[15] F. W. Low, C. W. Lai, K. M. Lee & J. C. Juan, "Enhance of TiO_2 dopants incorporated reduced graphene oxide via RF magnetron sputtering for efficient dye-sensitized solar cells," Rare Metals **37**, 11 (2018) 919-928.

[16] E. Nouri, M. Reza & P. Lianos, "Impact of preparation method of TiO_2-rGO nanocomposite photoanodes on the performance of dye-sensitized solar cells," Electrochimica Acta **219**, (2016) 38-48.

[17] H. Awang & N. I. Talahah, "Synthesis of Reduced Graphene Oxide-Titanium (rGO-TiO_2) Composite Using a Solvothermal and Hydrothermal Methods and Characterized via XRD and UV-Vis," Natural Resources **10**, 2 (2019) 17-28.

[18] H. Elbony, A. Thapa, P. Poudel, N. Adhikary, S. Venkatesan & Q. Qiao, "Vanadium Oxide as a new charge recombination blocking layer for high efficiency dye-sensitized solar cells," Nano Energy **13**, (2015) 368-375.

[19] R. Raja, M. Govindaraj, M. D. Antony, K. Krishnan, E. Velusamy, A. Sambandam, V. W. Rayar, "Effects of TiO_2/rGO composite thin film as a blocking layer on the efficiency of dye-sensitized solar cells," Journal of Solid State Electrochemistry **21**, 3 (2016) 891-903.
[20] B. Tang, H. Chen, H. Peng, Z. Wang & W. Huang, "Graphene Modified TiO_2 Composite Photocatalysts: Mechanism, Progress and Perspective," Nanomaterials **8**, 2 (2018) 105.
[21] Y. Zhang & C. Pan, "TiO_2/Graphene composite from thermal reaction of graphene oxide and its photocatalytic activity in visible light," Journal of Materials Science **46**, 8 (2010) 2622-2626.
[22] M. R. Hasan, S. B. Hamid, W. J. Basirun, S. H. M. Suhaimy & A. N. Che Mat, "A sol-gel derived, copper dioxide-reduced graphene oxide nanocomposite electrode for the photoelectrocatalytic reduction of CO_2 to methanol and formic acid," Royal Society of Chemistry **5**, (2015) 77803-77813.